https://doi.org/10.5194/tc-2020-107
Preprint. Discussion started: 8 June 2020
© Author(s) 2020. CC BY 4.0 License.

The Cryosphere Discussions
Open Access
EGU

The case of a southern European glacier disappearing under recent warming that survived Roman and Medieval warm periods

Ana Moreno[1], Miguel Bartolomé[2], Juan Ignacio López-Moreno[1], Jorge Pey[1,3], Pablo Corella[4], Jordi García-Orellana[5,6], Carlos Sancho[Ŧ], María Leunda[7], Graciela Gil-Romera[8,1], Penélope González-Sampériz[1], Carlos Pérez-Mejías[9], Francisco Navarro[10], Jaime Otero-García[10], Javier Lapazaran[10], Esteban Alonso-González[1], Cristina Cid[11], Jerónimo López-Martínez[12], Belén Oliva-Urcia[12], Sérgio Henrique Faria[13,14], María José Sierra[15], Rocío Millán[15], Xavier Querol[16], Andrés Alastuey[16] and José M. García-Ruíz[1]

1. Departamento de Procesos Geoambientales y Cambio Global, Instituto Pirenaico de Ecología – CSIC, 50059, Zaragoza, Spain
2. Departamento de Geología, Museo de Ciencias Naturales - CSIC, Madrid, 28034, Spain
3. Fundación Aragonesa para la Investigación y el Desarrollo, ARAID, Zaragoza, Spain
4. Université Grenoble Alpes, CNRS, IRD, Grenoble INP, IGE, 38000 Grenoble, France
5. Institut de Ciència i Tecnologia Ambientals, Universitat Autònoma de Barcelona, Barcelona, Spain
6. Departament de Física, Universitat Autònoma de Barcelona, Barcelona, Spain
7. Institute of Plant Sciences & Oeschger Centre for Climate Change Research. Altenbergrain 21, 3013 Bern, Switzerland
8. Department of Ecology, Faculty of Biology, Philipps-Marburg University, Marburg, Germany
9. Institute of Global Environmental Change, Xi'an Jiaotong University, Xi'an, 710049, China
10. Departamento de Matemática Aplicada a las TIC, ETSI de Telecomunicación, Universidad Politécnica de Madrid, Madrid, Spain
11. Centro de Astrobiología – CSIC-INTA, Madrid, Spain
12. Departamento de Geología y Geoquímica, Facultad de Ciencias, Universidad Autónoma de Madrid, Madrid, Spain
13. Basque Centre for Climate Change (BC3), 48940, Leioa, Spain
14. IKERBASQUE, Basque Foundation for Science, 48011, Bilbao, Spain
15. CIEMAT — Environmental Department (DMA), Avenida Complutense 40, E-28040 Madrid, Spain
16. Institute of Environmental Assessment and Water Research – CSIC, 08034 Barcelona, Spain

Ŧ Deceased

Corresponding author: Ana Moreno (amoreno@ipe.csic.es) ORCID: 0000-0001-7357-584X

Keywords

Pyrenees, mountain glacier, current global warming, Medieval Climate Anomaly

https://doi.org/10.5194/tc-2020-107
Preprint. Discussion started: 8 June 2020
© Author(s) 2020. CC BY 4.0 License.

The Cryosphere
Discussions
Open Access
EGU

Abstract

Mountain glaciers have generally experienced an accelerated retreat over the last three decades as a rapid response to current global warming. However, the response to previous warm periods in the Holocene is not well-described for glaciers of the of southern Europe mountain ranges, such as the Pyrenees. The situation during the Medieval Climate Anomaly (900-1300 CE) is particularly relevant since it is not certain whether the glaciers just experienced significant ice loss or whether they actually disappeared. We present here the first chronological study of a glacier located in the Central Pyrenees (N Spain), the Monte Perdido Glacier (MPG), carried out by different radiochronological techniques and their comparison with geochemical proxies with neighboring paleoclimate records. The result of the chronological model proves that the glacier endured during the Roman Period and the Medieval Climate Anomaly. The lack of ice from last 600 years indicates that the ice formed during the Little Ice Age has melted away. The analyses of the content of several metals of anthropogenic origin, such as Zn, Se, Cd, Hg, Pb, appear in low amounts in MPG ice, which further supports our age model in which the record from the industrial period is lost. This study confirms the exceptional warming of the last decades in the context of last two millennia. We demonstrate that we are facing an unprecedented retreat of the Pyrenean glaciers which survival is compromised beyond a few decades.

https://doi.org/10.5194/tc-2020-107
Preprint. Discussion started: 8 June 2020
© Author(s) 2020. CC BY 4.0 License.

The Cryosphere Discussions
Open Access
EGU

1. Introduction

Mountain glaciers are often sensitive to climate variations on temporal scales from decades to centuries. It is well known that summer temperature and winter precipitation are the most important climate parameters influencing glacier mass balance (Oerlemans, 2001). Therefore, continuous records of past glacier size fluctuations provide valuable information about the timing and magnitude of Holocene climate shifts (Solomina et al., 2015, 2016), which contributed to explain the characteristics and evolution of plant cover, human movements and land use. Several glacier advances during the Neoglacial (which started around 6000-5000 yr ago) have been identified and associated to sustained cooling periods across the North Atlantic (Wanner et al., 2011). The most recent period of global glacier expansion took place during the Little Ice Age (LIA), beginning in the 13th century and reaching a maximum between the 17th and 19th centuries (Solomina et al., 2016). Afterwards, most glaciers worldwide have retreated rapidly, as indicated by measurements of ice volume and ice-covered area, and this trend seems to have accelerated over the last three decades (Marzeion et al., 2014; Zemp et al., 2015, 2019).

Despite broad agreement on millennial-scale trends in global glacier fluctuations and Holocene climate variability (Davis et al., 2009; Solomina et al., 2015), regional variations are not so well constrained. For instance, for the Pyrenees, a mountain range that currently hosts the majority of the southernmost glaciers in Europe, there is a significant lack of knowledge about Holocene glacier fluctuations, as indicated scarce evidences of glacier advances during the Neoglacial period (García-Ruiz et al., 2014; Gellatly et al., 1992). Based on Pyrenean tree-ring chronologies, summer temperatures during the Medieval Climate Anomaly (MCA, circa 900–1300 CE) were estimated to be as warm as those of the 20th century (Büntgen et al., 2017), but no information has been obtained on the glacier response to MCA warming. Conversely, glacier advance during the LIA is well constrained in the Mediterranean mountains (García-Ruiz et al., 2014; González Trueba et al., 2008; Hughes, 2018; Oliva et al., 2018) and a significant deglaciation is also evident in recent times (López-Moreno et al., 2016; Rico et al., 2017). Thus, Pyrenean glaciers have exhibited during the 20th and 21st centuries multi-decadal variations similar to those of other mountain ranges in the world. In particular,

https://doi.org/10.5194/tc-2020-107
Preprint. Discussion started: 8 June 2020
© Author(s) 2020. CC BY 4.0 License.


the period from the 1980s to present has been the most intense in terms of number of glaciers that disappeared (from 39 inventoried Pyrenean glaciers in 1984 to 19 at present) (Rico et al., 2017). Given the small size of the Pyrenean glaciers and their current critical situation in the context of global warming, we hypothesize that they could have disappeared completely during the aforementioned warm periods

This study is focused on Monte Perdido Glacier, located in the Spanish Central Pyrenees, which is currently one of the best monitored small glaciers (<0.5 km^2) worldwide. Recent research based on different ground-based remote sensing techniques has demonstrated a rapid retreat of this glacier, with an average loss of ice thickness of about one meter per year since 1981 (López-Moreno et al., 2019). These results, together with the evidences of long-term retreat since the LIA glacier position indicated by pictures and moraines, suggest that this glacier could disappear over the next few decades (López-Moreno et al., 2016). The present study relies on a variety of dating techniques and on the analysis of several proxies associated to environmental and anthropogenic changes to construct, for the first time, the chronology of an ice sequence from a Pyrenean glacier. Such analyses will respond the key question of whether Pyrenean glaciers may have survived previous Holocene warm periods.

2. Study area

The Monte Perdido Glacier (MPG, 42°40′50″N; 0°02′15″E.) is located in the Central Spanish Pyrenees, in the Ordesa and Monte Perdido National Park (OMPNP) (Fig.1). It currently consists of two separate ice bodies, which were connected in the past. Both are north facing and lie on structural flats beneath the main summit of the Monte Perdido Peak (3355 m a.s.l.) and are surrounded by vertical cliffs of 500–800 m in height. At the base of the cliffs, the Cinca River flows directly from the glacier and the surrounding slopes, and has created a longitudinal west–east basin called the Marboré Cirque (5.8 km^2). This is the area within the Pyrenees with the highest variety of recent morainic deposits (García-Ruiz et al., 2014). Additionally, a a 6-m thick sediment core obtained in 2011 from a lake inside the cirque (Marboré Lake) contains valuale information from the last 14,600 years of the depositional evolution of the lake (Oliva-Urcia et al., 2018) and of the regional variations in the vegetation cover (Leunda et al.,

https://doi.org/10.5194/tc-2020-107
Preprint. Discussion started: 8 June 2020
© Author(s) 2020. CC BY 4.0 License.


2017). The Marboré Lake (2595 m a.s.l.) is located in the Marboré or Tucarroya Cirque, in the northern face of the Monte Perdido massif. The distance between the lake and the MPG is approximately 1300 m and, therefore, both have been affected by similar palaeoenvironmental conditions.

Recent measurements indicate that the total surface area of MP glacier in 2016 was 0.385 km^2 (López-Moreno et al., 2016). During the period 2011–2019, the glacier ice thickness decreased by 7.4 m on average, though such losses exhibit a marked spatial and temporal variability (Fig. S1, Supplementary Material). According to recent measurements of air temperature (July 2014 to October 2017), the 0 °C isotherm lies at 2945 m a.s.l., suggesting that the potential glacier accumulation area is very small, even inexistent during warm years. In an average summer (June to September; temperature measurements were conducted from 2014 to 2017), the temperature at the foot of the glacier is 7.3 °C. No direct observations of precipitation are available at the glacier location, but the maximum accumulation of snow in late April during the three available years was 3.23 m, and average snow density was 454 kg m^{-3} measured in the field, indicating that total water equivalent during the main accumulation period (October to April) could be close to 1500 mm (López-Moreno et al., 2019).

3. Material and methods

3.1. Ice sampling and storage

Ice drilling in MPG was carried out in September 2017 using a Kovacs ice coring device at three sites. These sites were selected based on previously obtained ground-penetrating radar (GPR) results, which, combined with glacier dynamics modelling, suggested that the oldest ice could be located at these locations since the thickness was over 30 m and there was no movement of the ice (López-Moreno et al., 2019) (Fig. 1). Unfortunately, none of the glacio-meteorological and topographical criteria required to obtain a preserved ice-core stratigraphy, such as low temperatures to prevent water percolation, or a large extension and flat surface topography to minimize the influence of glacier flow (Garzonio et al., 2018), are currently met in the glacier. With this technique, only three short ice cores of 4, 3 and 2 m in length could be recovered, which could not provide a complete chrono-stratigraphical ice sequence.

https://doi.org/10.5194/tc-2020-107
Preprint. Discussion started: 8 June 2020
© Author(s) 2020. CC BY 4.0 License.


149 The cores were preserved intact and later stored at −60 °C at the BC3-IzotzaLab ice
150 core facility (Leioa, Spain) but not used in this study.

151 Based on the poor core recovery, we changed our drilling strategy and, to collect ice
152 samples in an ordered chrono-stratigraphical sequence covering from the oldest to the
153 newest ice preserved in the glacier, we took samples in an area with no evidence of
154 current ice movement, as confirmed by results from interferometric radar and GNSS
155 measurements (López-Moreno et al., 2019) (Fig.S2). This sector has been eroded to
156 form a current steady slope of 20° where it is possible to establish a relation between
157 the sample distances and the ice depth in a formerly much less steep glacier surface.
158 Due to the small size of this glacier, the ice needs to be frozen to bedrock, and hence
159 nearly stagnant, to become of substantial age, i.e., a few hundred years or more, as
160 indicated by previous studies in similar glaciers Gabrielli et al., 2016; Haeberli et al.,
161 2004). Therefore, we measured one-meter thickness using the Jacob's staff at every
162 sampling point to measure stratigraphic thicknesses since bedding was unclear (Fig.
163 S2). Once cleaned the most superficial ice to avoid new ice formed recently, we
164 recovered at every sampling position 3–4 small cores (6 cm in diameter and 25 cm in
165 length) using a custom stainless steel crown adaptor on a cordless power drill (see Fig.
166 S2 in Supplementary Material). Following that sampling procedure we recovered a
167 total of 100 samples, every one constituted by 3-4 cylinders, which represent the
168 whole ice sequence in MP glacier. Those ice samples were stored in a freezer room in
169 Zaragoza and further analysed to obtain their chronology (combining ^{210}Pb, ^{137}Cs and
170 ^{14}C techniques) and their geochemical composition (trace element and Hg
171 concentrations) (see below).

172 *3.2. Dating by ^{210}Pb and ^{137}Cs.*

173 The isotope ^{137}Cs usually associated to the fallout from nuclear tests during the 1950s
174 and the 1960s, as well as the Chernobyl (1986) and Fukushima (2011) accidents was
175 investigated by γ-spectrometry in the uppermost five samples in MPG, but no trace
176 could be detected (Table S1 in Supplementary Material). This implies that all samples
177 are older than 60–65 years and therefore they were not exposed to the atmosphere
178 after 1950 CE. Another possibility that was discarded once we had ^{14}C dates, is that all

https://doi.org/10.5194/tc-2020-107
Preprint. Discussion started: 8 June 2020
© Author(s) 2020. CC BY 4.0 License.


samples were younger than 1950 CE. Additionally, up to ten samples were selected from the 100 samples that constitute the whole ice sequence to carry out ^{210}Pb analysis as an independent dating method to obtain chronologies for about the last hundred years of glacier ice (Eichler et al., 2000; Herren et al., 2013). Those samples were selected from the top of the sequence (Table S2). Determination of ^{210}Pb activities was accomplished through the measurement of its daughter nuclide, ^{210}Po, by α-spectrometry following the methodology described in (Sanchez-Cabeza et al., 1998) (Table S2 in Supplementary Material). Similarly, ^{210}Pb activity was also undetectable in most cases, except in three samples (MP100, MP73 and MP76) with concentrations above minimum detection activity (MDA; Table S2). Probably, the MP100 sample contained the ^{210}Pb recently deposited because it was the most superficial sample, therefore in contact with the atmosphere. However, this sample, as well as samples MP73 and MP76 contained a large amount of lithogenic particulate material from atmospheric dust or ash deposits. The absence of ^{210}Pb activity in the analysed samples does not allow constructing an age-depth model for the last 100 years indicating that MPG ice samples were very likely older and the ^{210}Pb had completely decayed. We then built up the proposed MPG chronology using AMS ^{14}C dating.

3.3.Dating by ^{14}C method.

Sixteen accelerator mass spectrometry (AMS) ^{14}C dates from MPG ice were obtained by combining bulk organic matter (9 samples), pollen concentrates (3 samples), bulk sediment accumulated in filters (2 filters), and water-insoluble organic carbon (WIOC) particles (2 samples) (Table 1). First, using a binocular microscope [x10], we selected organic particles for dating from the nine selected bulk samples, once the ice sample was melted. However, the small size prevented us from classifying the organic remains. All the amorphous particles were sent to the dating laboratory (Direct AMS, Seattle, USA). Pollen concentrates were prepared from three selected samples (30, 70 and 100 m depth) to complete the previous set of samples following the standard palynological method, including a chemical treatment and mineral separation in heavy liquid (Thoulet: density 2.0; Moore et al., 1991). Additionally, two ice samples previously melted (67 and 81 m depth) were filtered throughout a filtration line

https://doi.org/10.5194/tc-2020-107
Preprint. Discussion started: 8 June 2020
© Author(s) 2020. CC BY 4.0 License.


connected to a vacuum pump using 47 mm quartz fiber filters (PALL tissuquarzt 2500QAT-UP), parameterized at controlled conditions (temperature: 22–24 °C; relative humidity 25–35%) and weighted twice in different days. Abundant material was obtained, but no control was made on the composition and amount of organic material versus other type of inputs. Concentrated pollen samples and filters were dated at the same laboratory (Direct AMS, Seattle, USA). Since organic fragments (plants, wood, insects) are rarely found in mountain glaciers, a new, complementary dating tool was recently developed based on extracting the microgram-amounts of the water-insoluble organic carbon (WIOC) fraction of carbonaceous aerosols embedded in the ice matrix for subsequent ^{14}C dating (Uglietti et al., 2016). Two samples were dated by the WIOC technique at the Laboratory of Environmental Chemistry, Paul Scherrer Institute, Switzerland, following the usual procedures including removing the outer part of the ice core segment for decontamination purposes (Jenk et al., 2009).

Finally, from the initial 16 dates, we had to discard seven (see the criteria in section 4.1 below) and the age model was developed including nine samples (eight from bulk organic matter and one from the WIOC technique; Table 1). Those nine dates were converted into calendar ages by the CALIB 5.0.2 software, which uses the most updated dataset, INTCAL13 (Reimer et al., 2013) (Table 1). The median of the one-σ probability interval was selected for these dates, resulting in large errors (230 years on average) in the obtained calendar ages. The depth–age model was created using the R package CLAM 2.2 (Blaauw, 2010; Blaauw et al., 2019) (Fig. 2). Given the scattered depths at which dates concentrate, we chose to perform a non-smooth, second order polynomial regression for preventing any model over-fitting and a spurious age–depth relationship. In addition, we run the depth–age model setting a hiatus at 73 m depth where we think an interruption in the ice accumulation was produced. This idea is supported by the observation of several debris layers that increased their frequency towards the top of the glacier. Those layers are interpreted as the result of several phases of melting, dramatically changing the accumulation rates and concentrating samples of similar ages (see section 4.1 below). Full details on how the model was performed and a reproducible workflow with the current chronological dataset are available in the Supplementary Material.

https://doi.org/10.5194/tc-2020-107
Preprint. Discussion started: 8 June 2020
© Author(s) 2020. CC BY 4.0 License.

The Cryosphere
Discussions
Open Access
EGU

241 *3.4. Trace elements in soluble and insoluble material*.

242 35 selected ice samples from the altitudinal transect were melted and filtered through
243 a filtration ramp connected to a vacuum pump using 47 mm quartz fiber filters (PALL
244 tissuquarzt 2500QAT-UP). Filters were pre-heated at 250 °C and thereafter prepared in
245 controlled conditions (temperature: 22–24 °C; relative humidity: 25–35 %) before and
246 after filtration. Subsequently, they were weighted in two different days. Mass
247 difference between blank and sampled filters was used to calculate the amount of
248 insoluble material entrapped in ice samples. For every sample, an aliquot and a filter
249 were obtained. From aliquots, anions and cations, as well as major and trace elements
250 were determined. From filters, we determined major and trace elements, as well as
251 organic and elemental carbon, following the method devised by (Pey et al., 2013)
252 (Table 2). Basically, an acidic digestion (HNO_3:HF:$HClO_4$) of half of each filter was
253 conducted, driven to complete dryness, being the remaining material re-dissolved in
254 HNO_3. Inductively coupled plasma mass spectrometry (ICP-MS) and inductively
255 coupled plasma atomic emission spectroscopy (ICP-AES) were used to determine major
256 and trace elements. From the other half of each filter, a 1.5 cm^2 section was used to
257 determine Organic Carbon (OC) and Elemental Carbon (EC) concentrations by using a
258 SUNSET thermo-optical analyzer, following the EUSAAR_2 temperature protocol. Table
259 1 also contains the Enrichment Factors (EFs) calculated as follows:

260
$$EF_{iCODD} = \frac{X_{iCODD}/Al_{CODD}}{X_{iUC}/Al_{UC}} \qquad EF_{iMPGID} = \frac{X_{iMPGID}/Al_{MPGID}}{X_{iUC}/Al_{UC}} \qquad EF_{i} = \frac{X_{iCODD}/Al_{CODD}}{X_{iMPGID}/Al_{MPGID}}$$

261 where EF_{iCODD} is the Al-normalised Enrichment Factor with respect to the Upper Crust
262 (*UC*, (Taylor and McLennan, 1995)) of an *'i'* element in the current Ordesa's deposited
263 dust (*CODD*); EF_{iMPGID} is the Al-normalised Enrichment Factor with respect to the *UC* of
264 an *'i'* element in the current MPG ice dust (*MPGID*); and EF_i is the Al-normalised
265 Enrichment Factor with respect to *CODD* of an *'i'* element in the *MPGID*.

266 Regarding the Pb/Al ratio, we carried out a normalization with Al in both, ice and lake
267 records, to disentangle the anthropogenic lead variability from possible detrital inputs.

https://doi.org/10.5194/tc-2020-107
Preprint. Discussion started: 8 June 2020
© Author(s) 2020. CC BY 4.0 License.

The Cryosphere Discussions
Open Access
EGU

Aluminum has been selected for normalization since this lithogenic element is immobile and abundant in carbonated watersheds.

3.5. Hg determination.

Total Hg concentration measurements were carried out in 21 selected samples by Atomic Absorption Spectrophotometry using an Advance Mercury Analyzer (AMA 254, LECO Company). This equipment is specifically designed for direct mercury determination in solid and liquid samples without sample chemical pre-treatment. Certified reference materials were used to determine the accuracy and precision of the Hg measurements. These reference materials were ZC73027 (rice, 4.8 ± 0.8 µg kg^{-1}) and CRM051–050 (Clay soil, 4.08 ± 0.09 mg kg^{-1}). The repeatability was Sr ≤ 15 % and the relative uncertainty associated with the method (k = 2; confidence level of about 95%) was ±20 %. All analyses were run at least three times. Total metal concentrations were expressed in µg g^{-1} of dry weight sediment due to the low amount detected.

4. Results and discussion

4.1. Dating of ice from the Monte Perdido Glacier

Dating of ice cores from temperate, non-polar glaciers is challenging and often problematic as annual layer counting is precluded due to periods without net accumulation, and to ice deformation caused by glacier flow (Festi et al., 2016; Thompson et al., 2006). Hence, we have constrained the age of glacier ice within the last 100 years by using ^{210}Pb and ^{137}Cs relative dating methods, and for the oldest sections we used ^{14}C absolute dating from different materials (*Sect. Material and methods* and Tables S1, S2 in Supplementary Material). Additionally, characteristics of the ice stratigraphy, such as the presence of dark debris-rich layers, were integrated into the chronology. Finally, proxy comparison with independently dated sediments of the Marboré Lake located nearby (Corella et al., 2018; Oliva-Urcia et al., 2018) (Fig.1) helped to support the obtained MPG age-depth model .

We took most of the ice samples for dating in sections where dark debris layers alternated every ca. 5 m with cleaner and clearer ice (Fig. S2 in Supplementary Material). The debris layers were composed of detrital, silty-sandy size deposits, likely

https://doi.org/10.5194/tc-2020-107
Preprint. Discussion started: 8 June 2020
© Author(s) 2020. CC BY 4.0 License.


297 coming from wind-blown particles (e.g. black carbon-rich particles, dust) and from
298 erosive processes of the limestone catchment, including the fall of gravel-sized
299 particles from the surrounding cliffs. These debris layers contain more organic remains
300 than those formed by clear ice, making them ideal spots to find datable remains.
301 Interestingly, the frequency of debris layers increases towards the top of the glacier,
302 where these layers are most abundant. We consider the accumulation of debris layers
303 to be indicative of reduced ice accumulation and dominance of ablation periods. In
304 such situations, the detrital and organic material concentrates as the ice melts, giving
305 its characteristic dark colour to the ice layers.

306 The chronology for the last 100 years was not eventually constrained using ^{210}Pb and
307 ^{137}Cs as samples proved to be older than the decay period of both radionuclides
308 (Tables S1 and S2, Supplementary Material). Thus, the lack of ^{210}Pb activity indicated
309 the lack of ice formed during the last 100 years. Regarding the ^{14}C dated samples,
310 some sample limitations precluded the construction of a chronology (Table 1). The
311 sample from 48 m depth (D-AMS 025295) was the only one from the nine bulk organic
312 matter samples to be discarded due to probable contamination, since small plastic
313 debris coming from the painting used in the coring device were identified under the
314 microscope. From the two WIOC-dated samples, one was discarded (MP10m), as it had
315 too small amount of organic carbon (5.3 μg), thus providing too inaccurate results. The
316 other sample (MP59m), with higher organic carbon (28.7 μg), was incorporated into
317 the age model. The other two methods (pollen and filters) used to concentrate organic
318 matter to be dated by ^{14}C were, unfortunately, not successful. The three pollen
319 concentrates provided unreliably old datings. We hypothesize that these old datings
320 are likely associated to melting processes of older ice layers accumulated in the upper
321 ice body of MPG (Neoglacial or Roman times), which later percolated through the ice,
322 as observed in other glaciers (Ewing et al., 2014). Similarly, we discarded the two filter
323 samples from 67 m and 81 m depth (D-AMS 029894 and D-AMS 033972, respectively).
324 The material accumulated in the filters was a mixture of particles containing detrital
325 carbonate eroded from Eocene limestones or supplied by Saharan dust, which was not
326 removed and probably influenced the results incorporating dead carbon to the
327 samples.

https://doi.org/10.5194/tc-2020-107
Preprint. Discussion started: 8 June 2020
© Author(s) 2020. CC BY 4.0 License.


328 Finally, from the original set of sixteen absolute dates obtained, we selected the nine
329 samples which did not present any problem related to the amount of carbon, possible
330 contamination, material from different sources or percolation within the ice sequence.
331 These nine samples were all chrono-stratigraphically coherent (eight from bulk organic
332 matter and one from WIOC-technique). The age-depth model obtained indicates the
333 presence of ice since 2000 years ago and allows distinguishing three main periods for
334 MPG (Fig. 2). First, an accumulation period from 0 to 700 CE. Second, an ablation-
335 dominated phase from 700 to 1200 CE, which corresponds to the dark-rich layers
336 interval. Third, a new accumulation period from 1200 to 1400 CE. Finally, no ice
337 formed during, at least, the last 600 years has been found today in MPG according to
338 this age model. This indicates that the LIA ice has been melted away, thus
339 demonstrating an intense ablation period since 1850 CE. The MPG chronology is
340 supported by, first, a quantitative comparison with present-day atmospheric
341 particulate matter (Table 2) and, second, by the comparison with the
342 paleoenvironmental sequence of the Marboré Lake for the last 2000 years (Fig. 3) (see
343 text below).

344 We have used the averaged concentration values of major and trace elements
345 currently obtained at a monitoring station located in Ordesa and Monte Perdido
346 National Park (8 km away from the MPG, at 1190 m a.s.l.), where deposited
347 atmospheric particulate matter is sampled monthly (Table 2). Interestingly, the
348 elements that abound nowadays in the Ordesa station are not so abundant in the ice
349 from MPG. Indicators such as organic carbon, Zn, Se and Cd concentrations, all of
350 which are potential proxies of current anthropogenic emissions, are much higher in the
351 samples from Ordesa, which are representative of today's atmosphere, than in the ice
352 samples from the MPG. The low concentration of these elements in MPG samples
353 could indicate their disappearance from glacier surface layers due to its continuous
354 melting. This supports our suggested age model (Fig. 2), in which the industrial period
355 has not been recorded. Contrariwise, the Al-normalised enrichment factor (EF) of Ti,
356 Mn, Cr, Co, Ni, Cu and Pb, elements linked to the natural fraction (dust deposition,
357 lithogenic elements) and mining activities (Corella et al., 2018), are more abundant in
358 the MPG ice samples than in the present-day Ordesa aerosols (Table 2). From them, Cu

https://doi.org/10.5194/tc-2020-107
Preprint. Discussion started: 8 June 2020
© Author(s) 2020. CC BY 4.0 License.


and Pb were markedly enriched (by a factor >6) in the MPG ice samples compared with the current deposited aerosols in Ordesa station.

Following previous studies on present-day atmospheric particulate matter composition from natural, urban or industrial areas (Querol et al., 2007), the values of some elemental ratios (e.g. Cu/Mn, As/Se, Pb/Zn) help to determine the origin of the particulate matter accumulated today. The Ordesa site can accordingly be mostly defined as remote in terms of atmospheric deposition ("rural background") while the average composition of MPG ice samples could be defined as a site under the influence of Cu mining and smelting activities, due to the high values of the Cu/Mn, As/Se and Pb/Zn ratios. It is noteworthy that Cu, Ag, and Pb mining and smelting have been historically documented in Bielsa valley during pre-industrial times (Callén, 1996). Indeed, MPG is only 7 km east from some of the largest lead and silver ore deposits in the Pyrenees (historical mines of Parzan). The impact of ancient environmental pollution in high alpine environments is archived in the lacustrine sequence of the neighbouring Marboré Lake, providing first evidences of historical metal mining and processing activities during the Roman Period (RP) (Corella et al., 2018, 2020). Therefore, the enrichment of trace elements in MPG ice record most likely corresponds to mining activities during ancient times. Recently, an ice core record from the western Alps have also demonstrated the suitability of glacier ice to record local and regional mining and smelting activities during RP and pre-Roman times (Preunkert et al., 2019).

The comparison of Pb/Al ratios from the independently dated records of Marboré Lake and MPG (Fig. 3) shows a reasonable agreement, supporting the obtained age model for MPG ice. Particularly, the high Pb/Al values in both records between the 1^{st}-5^{th} centuries can be explained by increased Pb emissions related to the aforementioned regional mining and smelting activities during the RP. Maximum Pb/Al values have been found in several natural archives in the Central Pyrenees since the onset of Industrialization at 1800 CE as well as in other glacier ice core archives from the Alps (Corella et al., 2017, 2018). Thus, the lack of a Pb/Al peak in the upper sequence of the MPG again confirms the absence of the last two centuries in MP ice record. Similarly, the Hg concentration in the glacier is very stable throughout the ice sequence (Fig.3).

https://doi.org/10.5194/tc-2020-107
Preprint. Discussion started: 8 June 2020
© Author(s) 2020. CC BY 4.0 License.


Hg concentrations in other ice core records preserve an increase during the onset of Industrialization at 1800 CE with maximum values typically 3–10 times higher than preindustrial values (Cooke et al., 2020). In Marboré Lake, the mercury increase occurred over the last 500 years associated to the maximum activity in the Spanish Almaden mines during the Colonial Period (Corella et al., 2020). Again, these results, lacking an expected increase in Hg levels, support the age model from the MPG record where the last six centuries of ice deposition are missing.

4.2. Evolution of the Monte Perdido glacier over the last 2000 years

The analyzed ice from MPG provides remarkable information about the evolution of the glacier in the last two millennia, which deserves be considered in the regional context. Based on published results, the oldest paleoclimatic information in the Marboré Cirque comes from the Marboré Lake, since no glacier deposits corresponding to the Late Pleistocene have been found in the cirque (García-Ruiz et al., 2014). There is sedimentological evidence that the Marboré Lake was already ice-free at least since the onset of the Bølling period (Greenland Interstadial-1, 14,600 yr BP), when clastic sediments were deposited in the lake basin (Leunda et al., 2017; Oliva-Urcia et al., 2018). This is coherent with the nearby La Larri juxta-glacial sequence which showed that the main Pineta glacier had already retreated further up in the headwater by 13,245 ± 120 yr BP (Salazar et al., 2013). In fact, glaciological studies performed in the Central Pyrenees confirm the sudden retreat of glaciers during the Bølling period, when they were reduced to small ice tongues, cirque glaciers or rock glaciers (Palacios et al., 2017).

Like other glaciers all over the world (Davis et al., 2009; Solomina et al., 2015), MPG likely experienced numerous spatial fluctuations during the Holocene, although absolute dates directly obtained from moraines are uncertain. A single boulder was dated from the outermost moraine corresponding to the maximum glacier expansion since the Younger Dryas (recalculated at 6900 ± 800 ^{36}Cl yr BP) (García-Ruiz et al., 2020) in the Marboré Cirque. This is the oldest Holocene date available for glacial deposits in Spain (García-Ruiz et al., 2014), and indicates a glacier advance during the Neoglacial period (Fig. 4A). Other minor advances would have occurred in MPG prior to

https://doi.org/10.5194/tc-2020-107
Preprint. Discussion started: 8 June 2020
© Author(s) 2020. CC BY 4.0 License.


420 the LIA, as inferred from three polished surfaces dated at 3500 ± 400, 2500 ± 300 and
421 1100 ± 100 ^{36}Cl yr BP, indicating the occurrence of different deglaciation phases, and
422 therefore glacial re-advances prior to these dates (García-Ruiz et al., 2020). Most likely,
423 the voluminous moraine at the foot of the Monte Perdido Massif, which undoubtedly
424 was deposited during the LIA, incorporates minor moraines and till from prior
425 Neoglacial advances, as has been reported in other Pyrenean cirques (Crest et al.,
426 2017; Palacios et al., 2017).

427 With the new chronology of the MPG record, we can ascertain that MPG has persisted
428 at least since the RP (circa 2000 yr ago). At that time, which is a well known warm
429 period in the Iberian Peninsula as recorded in both continental (Martín-Puertas et al.,
430 2010; Morellón et al., 2009) and marine sequences (Cisneros et al., 2016; Frigola et al.,
431 2007; Nieto-Moreno et al., 2011), the glacier was still active, but probably smaller than
432 during Neoglacial times (Fig. 4B). This situation probably continued during the
433 following cold period, the Dark Ages (DA, Fig 4C) when the glacier advanced as
434 indicated by the polished surface dated at 1100 ± 100 ^{36}Cl yr BP (García-Ruiz et al.,
435 2020). In glaciers in the Alps, reconstructions based on dating trees found within and
436 at the edge of glacier forefields have revealed a minimum glacier extent during the
437 Iron Age and the RP (Holzhauser et al., 2005), when glaciers were estimated to be
438 smaller than during the 1920s (Ivy-Ochs et al., 2009). Afterwards, in the late RP and the
439 early Middle Ages numerous glaciers in the Alps advanced during the DA, also known
440 as the Göschener II oscillation (Holzhauser et al., 2005).

441 The MCA (900–1300 CE) is the most recent preindustrial warm era in Europe (Mann et
442 al., 2009). For instance, in the Alps, a general glacier retreat has been observed during
443 this period, mainly associated with a decline in precipitation (Holzhauser et al., 2005).
444 According to the age-depth model, the MPG experienced a spectacular retreat (Fig.
445 4D), including the complete melting of some minor glaciers in the Marboré Cirque
446 (García-Ruiz et al., 2020). Nevertheless, during the MCA part of MPG was preserved, as
447 we find ice from 0 to 700 CE. No doubt the ice loss was significant, as evidenced by the
448 accumulation of dark strata over a long time interval (600–1200 CE) (Fig.2). On this
449 basis, we propose that the MPG was dominated by ablation processes during the MCA,
450 leading to considerable ice loss as deduced from just six meters of ice remaining from

https://doi.org/10.5194/tc-2020-107
Preprint. Discussion started: 8 June 2020
© Author(s) 2020. CC BY 4.0 License.


this period (Fig. 2). We assume that, by this time, basal ice of Neoglacial age was already removed, but at the end of the MCA the MPG still preserved ice from the RP and the first half of the DA (Fig. 4D).

Over such a diminished MCA glacier, ice started to accumulate again at a rapid rate during the LIA (1300–1850 CE). In most cases, the LIA was the period when mountain glaciers recorded their maximum Holocene extent (Solomina et al., 2016), with remarkable advances in the alpine glaciers (Ivy-Ochs et al., 2009). From a large variety of proxies, several warm and cold periods have been identified in the Iberian Peninsula during the LIA (Oliva et al., 2018). In the Marboré Cirque two generations of LIA moraines have been mapped (García-Ruiz et al., 2014), whose emplacement coincided with the coldest LIA phases, i.e. 1620-1715 CE, when the Pyrenean glaciers recorded their maximum extent, and 1820-1840 CE, when a rapid advance of the ice mass moved over the large moraine leaving parallel furrows, or flutes, as signs of erosion (García-Ruiz et al., 2020; Serrano and Martín-Moreno, 2018). These two cold phases are very well identified in the Marboré Cirque and were confirmed by the study of the altitudinal fluctuations of the timberline in the neighboring Escuaín Valley (Camarero et al., 2015). In fact, according to the map of Schrader from 1874 CE and other historical sources, the MPG made direct contact with the large moraine in the second half of the 19th century (García-Ruiz et al., 2014). Despite the MPG would have covered an area of 5.56 km^2 at the end of the LIA (in 1894, (González Trueba et al., 2008), Fig. 4E), there is no record today of ice accumulated during the LIA, except for a few meters at the top of the sequence corresponding to about 1400 CE. This means that more than 600 years of ice accumulation have been lost associated to the warming after ca. 1850 CE. This situation is not so common in the Alps, where ice from the LIA, and even from the last two centuries, is still preserved in many studied glaciers (Eichler et al., 2000; Gabrielli et al., 2016; Gäggeler et al., 1983; Preunkert et al., 2019).

Today the MPG is divided in two small ice bodies that together cover just 0.38 km^2 (López-Moreno et al., 2016, Fig. 4F). Comparing the MPG extent at the end of the LIA (ca. 1850 CE), thanks to the moraine location, and today, more than 5 km^2 of MPG would have disappeared, thus indicating that the last 150 years have likely been the period with the largest glacier melting in the last 2000 years.

https://doi.org/10.5194/tc-2020-107
Preprint. Discussion started: 8 June 2020
© Author(s) 2020. CC BY 4.0 License.


5. Conclusions

This study presents for the first time the chronology of a glacier in the Pyrenees, reconstructed from a set of ^{14}C dates on different organic remains and supported by measurements on current atmospheric deposition and comparison with a nearby lake sequence (Marboré Lake). The ice sequence from MPG covers the last 2000 years allowing defining cold periods of ice advance and warm periods of retreat. We demonstrate that the glacier was active during the RP, a well known warm period in Iberia Peninsula. During the MCA, the MPG experienced a spectacular retreat marked by the presence of dark debris layers indicative of successive years when ablation processes predominated. The LIA was a period of glacier advance but not recorded today in the ice from MPG since more than 600 years of ice accumulation have been lost associated to the warming after ca. 1850 CE. This evidence from the age-depth model is supported by the lack of anthropogenic indicators usually associated to the Industrial Era abundant today in current atmospheric deposition in a nearby site. Additionally, both Hg concentration and Pb/Al ratio appear much higher in the Marboré Lake sediments whereas they don't reflect the anthropogenic increase in the MPG record.

Comparing the present-day glacier situation with that of previous warm intervals, such as the RP or the MCA, we conclude that the MPG is nowadays greatly reduced in area and volume. Additionally, the recent ice mass loss rate is definitely more rapid than during the four centuries spanned by the MCA, thus suggesting that present day warming in the Pyrenees is faster and more intense than in any previous warm phase occurred during the last 2000 years. Under such climatic conditions, it is reasonable to expect the disappearance of this glacier, as well as other glaciers in the Pyrenees and in Southern Europe, over the next few decades.

6. Data availability

The input data file for CLAM, as well as the output results are stored in this journal for reviewing process and will be permanently deposited in the journal upon the acceptance of this manuscript. The other data are included in the tables and in the Supplementary.

https://doi.org/10.5194/tc-2020-107
Preprint. Discussion started: 8 June 2020
© Author(s) 2020. CC BY 4.0 License.


7. Author contributions

The paper was conceived by A.M., M.B., C.S. and J.I.L.M. and F.N., J.O.G., J.L., P.G.S., C.C., J. L.M., B.O., S.H.F and J.G.R. contributed to design this research project. J.G.O. carried out the ^{210}Pb and ^{137}Cs analyses; J.P., X.Q. and A.A. provided the geochemical data from Ordesa site and MPG; P.C., M.J.S. and R.M. provided the Hg data from Marboré Lake and MPG, C.P., M.L., E.A. helped during field work and G.G.R. run the R package CLAM 2.2 to build the age model. All authors contributed to the writing of the paper.

8. Competing interest

The authors declare that they have no conflict of interest.

9. Acknowledgements

The Spanish Agencia Estatal de Investigación (AEI – Spain) and the European Funds for Regional Development (FEDER – European Union) are gratefully acknowledged for financial support through PaleoICE EXPLORA project (CGL2015-72167-EXP), CGL2015-68993-R, CGL2015-69160-R and CTM2017-84441-R projects (AEI/FEDER, UE). SHF acknowledges support by the Spanish Government through María de Maeztu excellence accreditation 2018-2022 (MDM-2017-0714) and through the iMechPro RETOS project (RTI2018-100696-B-I00). M.B is supported by postdoctoral fellowship Juan de la Cierva-Formación program provided by the Spanish Ministry (ref.: FJCI-2017-34235063753). The authors are grateful to Eduardo Bartolomé and José Estebán Lozano for their help manufacturing parts of the coring devices and to the support provided by the "Dirección General de Conservación del Medio Natural (Government of Aragón)" and to the staff of the Ordesa and Monte Perdido National Park during our field campaigns.

10. References

Blaauw, M.: Methods and code for 'classical' age-modelling of radiocarbon sequences, Quaternary Geochronology, 5(5), 512–518, doi:10.1016/j.quageo.2010.01.002, 2010.

Blaauw, M., Christen, J. A., Vázquez, J. E. and Goring, S.: clam: Classical Age-Depth Modelling of Cores from Deposits. CRAN 2019, [online] Available from: https://CRAN.R-project.org/package=clam, 2019.

https://doi.org/10.5194/tc-2020-107
Preprint. Discussion started: 8 June 2020
© Author(s) 2020. CC BY 4.0 License.

542 Büntgen, U., Krusic, P. J., Verstege, A., Sangüesa-Barreda, G., Wagner, S., Camarero, J. J.,
543 Ljungqvist, F. C., Zorita, E., Oppenheimer, C., Konter, O., Tegel, W., Gärtner, H., Cherubini, P.,
544 Reinig, F. and Esper, J.: New Tree-Ring Evidence from the Pyrenees Reveals Western
545 Mediterranean Climate Variability since Medieval Times, J. Climate, 30(14), 5295–5318,
546 doi:10.1175/JCLI-D-16-0526.1, 2017.

547 Callén, J. J. N.: El proceso sidero-metarlúrgico altoaragonés: los valles de Bielsa y Gistain en la
548 Edad Moderna (1565-1800), Llull: Revista de la Sociedad Española de Historia de las Ciencias y
549 de las Técnicas, 19(37), 471–508, 1996.

550 Camarero, J. J., García-Ruiz, J. M., Sangüesa-Barreda, G., Galván, J. D., Alla, A. Q., Sanjuán, Y.,
551 Beguería, S. and Gutiérrez, E.: Recent and Intense Dynamics in a Formerly Static Pyrenean
552 Treeline, Arctic, Antarctic, and Alpine Research, 47(4), 773–783, doi:10.1657/AAAR0015-001,
553 2015.

554 Cisneros, M., Cacho, I., Frigola, J., Canals, M., Masqué, P., Martrat, B., Casado, M., Grimalt, J.
555 O., Pena, L. D., Margaritelli, G. and Lirer, F.: Sea surface temperature variability in the central-
556 western Mediterranean Sea during the last 2700 years: a multi-proxy and multi-record
557 approach, Clim. Past, 12(4), 849–869, doi:10.5194/cp-12-849-2016, 2016.

558 Cooke, C. A., Martínez-Cortizas, A., Bindler, R. and Sexauer Gustin, M.: Environmental archives
559 of atmospheric Hg deposition – A review, Science of The Total Environment, 709, 134800,
560 doi:10.1016/j.scitotenv.2019.134800, 2020.

561 Corella, J. P., Valero-Garcés, B. L., Wang, F., Martínez-Cortizas, A., Cuevas, C. A. and Saiz-Lopez,
562 A.: 700 years reconstruction of mercury and lead atmospheric deposition in the Pyrenees (NE
563 Spain), Atmospheric Environment, 155, 97–107, doi:10.1016/j.atmosenv.2017.02.018, 2017.

564 Corella, J. P., Saiz-Lopez, A., Sierra, M. J., Mata, M. P., Millán, R., Morellón, M., Cuevas, C. A.,
565 Moreno, A. and Valero-Garcés, B. L.: Trace metal enrichment during the Industrial Period
566 recorded across an altitudinal transect in the Southern Central Pyrenees, Science of The Total
567 Environment, 645, 761–772, doi:10.1016/j.scitotenv.2018.07.160, 2018.

568 Corella, J. P., Sierra, M. J., Garralón, A., Millán, R., Rodríguez-Alonso, J., Mata, M. P., Wilhem,
569 B., Vivez, P., Duval, B., Amouroux, D., Vicente de Vera, A., Moreno, A., Cuevas, C. A., Adame, J.
570 A., Saiz-Lopez, A. and Valero Garcés, B.: Legacy pollution from roman and medieval mining in
571 the Iberian Peninsula recorded in high mountain ecosystems, Science of The Total
572 Environment, under review, 2020.

573 Crest, Y., Delmas, M., Braucher, R., Gunnell, Y. and Calvet, M.: Cirques have growth spurts
574 during deglacial and interglacial periods: Evidence from 10Be and 26Al nuclide inventories in
575 the central and eastern Pyrenees, Geomorphology, 278, 60–77,
576 doi:10.1016/j.geomorph.2016.10.035, 2017.

577 Davis, P. T., Menounos, B. and Osborn, G.: Holocene and latest Pleistocene alpine glacier
578 fluctuations: a global perspective, Quaternary Science Reviews, 28(21–22), 2021–2033,
579 doi:10.1016/j.quascirev.2009.05.020, 2009.

580 Eichler, A., Schwikowski, M., Gäggeler, H. W., Furrer, V., Synal, H.-A., Beer, J., Saurer, M. and
581 Funk, M.: Glaciochemical dating of an ice core from upper Grenzgletscher (4200 m a.s.l.),
582 Journal of Glaciology, 46(154), 507–515, doi:10.3189/172756500781833098, 2000.

https://doi.org/10.5194/tc-2020-107
Preprint. Discussion started: 8 June 2020
© Author(s) 2020. CC BY 4.0 License.


583 Ewing, M. E., Reese, C. A. and Nolan, M. A.: The potential effects of percolating snowmelt on
584 palynological records from firn and glacier ice, Journal of Glaciology, 60(222), 661–669,
585 doi:10.3189/2014JoG13J158, 2014.

586 Festi, D., Carturan, L., Kofler, W., dalla Fontana, G., de Blasi, F., Cazorzi, F., Bucher, E., Mair, V.,
587 Gabrielli, P. and Oeggl, K.: Linking pollen deposition, snow accumulation and isotopic
588 composition on the Alto dell'Ortles glacier (South Tyrol, Italy) for sub-seasonal dating of a firn
589 temperate core, The Cryosphere Discussions, 1–16, doi:10.5194/tc-2016-221, 2016.

590 Frigola, J., Moreno, A., Cacho, I., Canals, M., Sierro, F. J., Flores, J. A., Grimalt, J. O., Hodell, D. A.
591 and Curtis, J. H.: Holocene climate variability in the western Mediterranean region from a
592 deepwater sediment record, Paleoceanography, 22(doi:10.1029/2006PA001307), 2007.

593 Gabrielli, P., Barbante, C., Bertagna, G., Bertó, M., Binder, D., Carton, A., Carturan, L., Cazorzi,
594 F., Cozzi, G., Dalla Fontana, G., Davis, M., De Blasi, F., Dinale, R., Dragà, G., Dreossi, G., Festi, D.,
595 Frezzotti, M., Gabrieli, J., Galos, S. P., Ginot, P., Heidenwolf, P., Jenk, T. M., Kehrwald, N.,
596 Kenny, D., Magand, O., Mair, V., Mikhalenko, V., Lin, P. N., Oeggl, K., Piffer, G., Rinaldi, M.,
597 Schotterer, U., Schwikowski, M., Seppi, R., Spolaor, A., Stenni, B., Tonidandel, D., Uglietti, C.,
598 Zagorodnov, V., Zanoner, T. and Zennaro, P.: Age of the Mt. Ortles ice cores, the Tyrolean
599 Iceman and glaciation of the highest summit of South Tyrol since the Northern Hemisphere
600 Climatic Optimum, The Cryosphere, 10(6), 2779–2797, doi:10.5194/tc-10-2779-2016, 2016.

601 Gäggeler, H., Gunten, H. R. von, Rössler, E., Oeschger, H. and Schotterer, U.: 210Pb-Dating of
602 Cold Alpine Firn/Ice Cores From Colle Gnifetti, Switzerland, Journal of Glaciology, 29(101),
603 165–177, doi:10.1017/S0022143000005220, 1983.

604 García-Ruiz, J. M., Palacios, D., Andrés, N. de, Valero-Garcés, B. L., López-Moreno, J. I. and
605 Sanjuán, Y.: Holocene and 'Little Ice Age' glacial activity in the Marboré Cirque, Monte Perdido
606 Massif, Central Spanish Pyrenees, The Holocene, 24(11), 1439–1452,
607 doi:10.1177/0959683614544053, 2014.

608 García-Ruiz, J.M., Palacios, D., Andrés, N., López-Moreno, J.I.: Neoglaciation in the Spanish
609 Pyrenees: A multiproxy challenge. Mediterranean Geoscience Reviews.
610 https://doi.org/10.1007/s42990-020-00022-9, 2020.

611 Garzonio, R., Di Mauro, B., Strigaro, D., Rossini, M., Colombo, R., De Amicis, M. and Maggi, V.:
612 Mapping the suitability for ice-core drilling of glaciers in the European Alps and the Asian High
613 Mountains, J. Glaciol., 64(243), 12–26, doi:10.1017/jog.2017.75, 2018.

614 Gellatly, A. F., Grove, J. M. and Switsur, V. R.: Mid-Holocene glacial activity in the Pyrenees, The
615 Holocene, 2(3), 266–270, doi:10.1177/095968369200200309, 1992.

616 González Trueba, J. J., Moreno, R. M., Martínez de Pisón, E. and Serrano, E.: `Little Ice Age'
617 glaciation and current glaciers in the Iberian Peninsula, The Holocene, 18(4), 551–568,
618 doi:10.1177/0959683608089209, 2008.

619 Haeberli, W., Frauenfelder, R., Kääb, A. and Wagner, S.: Characteristics and potential climatic
620 significance of "miniature ice caps" (crest- and cornice-type low-altitude ice archives), Journal
621 of Glaciology, 50(168), 129–136, doi:10.3189/172756504781830330, 2004.

622 Herren, P.-A., Eichler, A., Machguth, H., Papina, T., Tobler, L., Zapf, A. and Schwikowski, M.: The
623 onset of Neoglaciation 6000 years ago in western Mongolia revealed by an ice core from the

© Author(s) 2020. CC BY 4.0 License.


624 Tsambagarav mountain range, Quaternary Science Reviews, 69, 59–68,
625 doi:10.1016/j.quascirev.2013.02.025, 2013.

626 Holzhauser, H., Magny, M. and Zumbühl, H. J.: Glacier and lake-level variations in west-central
627 Europe over the last 3500 years, The Holocene, 15(6), 789–801, 2005.

628 Hughes, P. D.: Little Ice Age glaciers and climate in the Mediterranean mountains: a new
629 analysis, CIG, 44(1), 15, doi:10.18172/cig.3362, 2018.

630 Ivy-Ochs, S., Kerschner, H., Maisch, M., Christl, M., Kubik, P. W. and Schlüchter, C.: Latest
631 Pleistocene and Holocene glacier variations in the European Alps, Quaternary Science Reviews,
632 28(21–22), 2137–2149, 2009.

633 Jenk, T. M., Szidat, S., Bolius, D., Sigl, M., Gäggeler, H. W., Wacker, L., Ruff, M., Barbante, C.,
634 Boutron, C. F. and Schwikowski, M.: A novel radiocarbon dating technique applied to an ice
635 core from the Alps indicating late Pleistocene ages, Journal of Geophysical Research:
636 Atmospheres, 114(D14), doi:10.1029/2009JD011860, 2009.

637 Leunda, M., González-Sampériz, P., Gil-Romera, G., Aranbarri, J., Moreno, A., Oliva-Urcia, B.,
638 Sevilla-Callejo, M. and Valero-Garcés, B.: The Late-Glacial and Holocene Marboré Lake
639 sequence (2612m a.s.l., Central Pyrenees, Spain): Testing high altitude sites sensitivity to
640 millennial scale vegetation and climate variability, Global and Planetary Change, 157, 214–231,
641 doi:10.1016/j.gloplacha.2017.08.008, 2017.

642 López-Moreno, J. I., Revuelto, J., Rico, I., Chueca-Cía, J., Julián, A., Serreta, A., Serrano, E.,
643 Vicente-Serrano, S. M., Azorin-Molina, C., Alonso-González, E. and García-Ruiz, J. M.: Thinning
644 of the Monte Perdido Glacier in the Spanish Pyrenees since 1981, The Cryosphere, 10(2), 681–
645 694, doi:10.5194/tc-10-681-2016, 2016.

646 López-Moreno, J. I., Alonso-González, E., Monserrat, O., Del Río, L. M., Otero, J., Lapazaran, J.,
647 Luzi, G., Dematteis, N., Serreta, A., Rico, I., Serrano-Cañadas, E., Bartolomé, M., Moreno, A.,
648 Buisan, S. and Revuelto, J.: Ground-based remote-sensing techniques for diagnosis of the
649 current state and recent evolution of the Monte Perdido Glacier, Spanish Pyrenees, J. Glaciol.,
650 65(249), 85–100, doi:10.1017/jog.2018.96, 2019.

651 Mann, M. E., Zhang, Z., Rutherford, S., Bradley, R. S., Hughes, M. K., Shindell, D., Ammann, C.,
652 Faluvegi, G. and Ni, F.: Global Signatures and Dynamical Origins of the Little Ice Age and
653 Medieval Climate Anomaly, Science, 326(5957), 1256–1260, 2009.

654 Martín-Puertas, C., Jiménez-Espejo, F., Martínez-Ruiz, F., Nieto-Moreno, V., Rodrigo, M., Mata,
655 M. P. and Valero-Garcés, B. L.: Late Holocene climate variability in the southwestern
656 Mediterranean region: an integrated marine and terrestrial geochemical approach, Clim. Past,
657 6(6), 807–816, doi:10.5194/cp-6-807-2010, 2010.

658 Marzeion, B., Cogley, J. G., Richter, K. and Parkes, D.: Attribution of global glacier mass loss to
659 anthropogenic and natural causes, Science, 345(6199), 919–921,
660 doi:10.1126/science.1254702, 2014.

661 Moore, P. D., Webb, J. A. and Collinson, M. E.: Pollen Analysis, Second., Blackwell Scientific
662 Publications., 1991.

663 Morellón, M., Valero-Garcés, B., Vegas-Vilarrúbia, T., González-Sampériz, P., Romero, Ó.,
664 Delgado-Huertas, A., Mata, P., Moreno, A., Rico, M. and Corella, J. P.: Lateglacial and Holocene

https://doi.org/10.5194/tc-2020-107
Preprint. Discussion started: 8 June 2020
© Author(s) 2020. CC BY 4.0 License.


665 palaeohydrology in the western Mediterranean region: The Lake Estanya record (NE Spain),
666 Quaternary Science Reviews, 28(25–26), 2582–2599, 2009.

667 Nieto-Moreno, V., Martínez-Ruiz, F., Giralt, S., Jiménez-Espejo, F., Gallego-Torres, D., Rodrigo-
668 Gámiz, M., García-Orellana, J., Ortega-Huertas, M. and de Lange, G. J.: Tracking climate
669 variability in the western Mediterranean during the Late Holocene: a multiproxy approach,
670 Clim. Past Discuss., 7(1), 635–675, doi:10.5194/cpd-7-635-2011, 2011.

671 Oerlemans, J.: Glaciers and Climate Change, CRC Press., 2001.

672 Oliva, M., Ruiz-Fernández, J., Barriendos, M., Benito, G., Cuadrat, J. M., Domínguez-Castro, F.,
673 García-Ruiz, J. M., Giralt, S., Gómez-Ortiz, A., Hernández, A., López-Costas, O., López-Moreno,
674 J. I., López-Sáez, J. A., Martínez-Cortizas, A., Moreno, A., Prohom, M., Saz, M. A., Serrano, E.,
675 Tejedor, E., Trigo, R., Valero-Garcés, B. and Vicente-Serrano, S. M.: The Little Ice Age in Iberian
676 mountains, Earth-Science Reviews, 177, 175–208, doi:10.1016/j.earscirev.2017.11.010, 2018.

677 Oliva-Urcia, B., Moreno, A., Leunda, M., Valero-Garcés, B., González-Sampériz, P., Gil-Romera,
678 G., Mata, M. P. and Group, H.: Last deglaciation and Holocene environmental change at high
679 altitude in the Pyrenees: the geochemical and paleomagnetic record from Marboré Lake (N
680 Spain), J Paleolimnol, 59(3), 349–371, doi:10.1007/s10933-017-0013-9, 2018.

681 Palacios, D., García-Ruiz, J. M., Andrés, N., Schimmelpfennig, I., Campos, N., Léanni, L.,
682 Aumaître, G., Bourlès, D. L. and Keddadouche, K.: Deglaciation in the central Pyrenees during
683 the Pleistocene–Holocene transition: Timing and geomorphological significance, Quaternary
684 Science Reviews, 162, 111–127, doi:10.1016/j.quascirev.2017.03.007, 2017.

685 Pey, J., Pérez, N., Cortés, J., Alastuey, A. and Querol, X.: Chemical fingerprint and impact of
686 shipping emissions over a western Mediterranean metropolis: Primary and aged contributions,
687 Science of The Total Environment, 463–464, 497–507, doi:10.1016/j.scitotenv.2013.06.061,
688 2013.

689 Preunkert, S., McConnell, J. R., Hoffmann, H., Legrand, M., Wilson, A. I., Eckhardt, S., Stohl, A.,
690 Chellman, N. J., Arienzo, M. M. and Friedrich, R.: Lead and Antimony in Basal Ice From Col du
691 Dome (French Alps) Dated With Radiocarbon: A Record of Pollution During Antiquity,
692 Geophysical Research Letters, 46(9), 4953–4961, doi:10.1029/2019GL082641, 2019.

693 Querol, X., Viana, M., Alastuey, A., Amato, F., Moreno, T., Castillo, S., Pey, J., de la Rosa, J.,
694 Sánchez de la Campa, A., Artíñano, B., Salvador, P., García Dos Santos, S., Fernández-Patier, R.,
695 Moreno-Grau, S., Negral, L., Minguillón, M. C., Monfort, E., Gil, J. I., Inza, A., Ortega, L. A.,
696 Santamaría, J. M. and Zabalza, J.: Source origin of trace elements in PM from regional
697 background, urban and industrial sites of Spain, Atmospheric Environment, 41(34), 7219–7231,
698 doi:10.1016/j.atmosenv.2007.05.022, 2007.

699 Reimer, P. J., Bard, E., Bayliss, A., Beck, J. W., Blackwell, P. G., Ramsey, C. B., Buck, C. E., Cheng,
700 H., Edwards, R. L., Friedrich, M. and others: IntCal13 and Marine13 radiocarbon age calibration
701 curves 0–50,000 years cal BP, Radiocarbon, 55(4), 1869–1887, 2013.

702 Rico, I., Izagirre, E., Serrano, E. and López-Moreno, J. I.: Superficie glaciar actual en los Pirineos:
703 Una actualización para 2016, Pirineos, 172(0), 029, doi:10.3989/Pirineos.2017.172004, 2017.

704 Salazar, A., Mata, M. P., Rico, M., Valero-Garcés, Oliva-Urcia, B. and Rubio, F. M.: El paleolago
705 de La Larri (Valle de Pineta, Pirineos), Cuadernos de Investigación Geográfica, 39(1), 97–116,
706 2013.

https://doi.org/10.5194/tc-2020-107
Preprint. Discussion started: 8 June 2020
© Author(s) 2020. CC BY 4.0 License.


707 Sanchez-Cabeza, J. A., Masqué, P. and Ani-Ragolta, I.: 210Pb and210Po analysis in sediments
708 and soils by microwave acid digestion, J Radioanal Nucl Chem, 227(1), 19–22,
709 doi:10.1007/BF02386425, 1998.

710 Serrano, E. and Martín-Moreno, R.: Surge glaciers during the Little Ice Age in the Pyrenees,
711 Cuadernos de Investigación Geográfica, 44(1), 213–244, doi:10.18172/cig.3399, 2018.

712 Solomina, O. N., Bradley, R. S., Hodgson, D. A., Ivy-Ochs, S., Jomelli, V., Mackintosh, A. N.,
713 Nesje, A., Owen, L. A., Wanner, H., Wiles, G. C. and Young, N. E.: Holocene glacier fluctuations,
714 Quaternary Science Reviews, 111, 9–34, doi:10.1016/j.quascirev.2014.11.018, 2015.

715 Solomina, O. N., Bradley, R. S., Jomelli, V., Geirsdottir, A., Kaufman, D. S., Koch, J., McKay, N. P.,
716 Masiokas, M., Miller, G., Nesje, A., Nicolussi, K., Owen, L. A., Putnam, A. E., Wanner, H., Wiles,
717 G. and Yang, B.: Glacier fluctuations during the past 2000 years, Quaternary Science Reviews,
718 149, 61–90, doi:10.1016/j.quascirev.2016.04.008, 2016.

719 Taylor, S. R. and McLennan, S. M.: The geochemical evolution of the continental crust, Reviews
720 of Geophysics, 33, 241–265, 1995.

721 Thompson, L. G., Mosley-Thompson, E., Brecher, H., Davis, M., Leon, B., Les, D., Lin, P.-N.,
722 Mashiotta, T. and Mountain, K.: Abrupt tropical climate change: Past and present, Proceedings
723 of the National Academy of Sciences, 103(28), 10536–10543, doi:10.1073/pnas.0603900103,
724 2006.

725 Uglietti, C., Zapf, A., Jenk, T. M., Sigl, M., Szidat, S., Salazar, G. and Schwikowski, M.:
726 Radiocarbon dating of glacier ice: overview, optimisation, validation and potential, The
727 Cryosphere, 10(6), 3091–3105, doi:10.5194/tc-10-3091-2016, 2016.

728 Wanner, H., Solomina, O., Grosjean, M., Ritz, S. P. and Jetel, M.: Structure and origin of
729 Holocene cold events, Quaternary Science Reviews, 30(21–22), 3109–3123,
730 doi:10.1016/j.quascirev.2011.07.010, 2011.

731 Zemp, M., Frey, H., Gärtner-Roer, I., Nussbaumer, S. U., Hoelzle, M., Paul, F., Haeberli, W.,
732 Denzinger, F., Ahlstrøm, A. P., Anderson, B., Bajracharya, S., Baroni, C., Braun, L. N., Cáceres, B.
733 E., Casassa, G., Cobos, G., Dávila, L. R., Granados, H. D., Demuth, M. N., Espizua, L., Fischer, A.,
734 Fujita, K., Gadek, B., Ghazanfar, A., Hagen, J. O., Holmlund, P., Karimi, N., Li, Z., Pelto, M., Pitte,
735 P., Popovnin, V. V., Portocarrero, C. A., Prinz, R., Sangewar, C. V., Severskiy, I., Sigurđsson, O.,
736 Soruco, A., Usubaliev, R. and Vincent, C.: Historically unprecedented global glacier decline in
737 the early 21st century, Journal of Glaciology, 61(228), 745–762, doi:10.3189/2015JoG15J017,
738 2015.

739 Zemp, M., Huss, M., Thibert, E., Eckert, N., McNabb, R., Huber, J., Barandun, M., Machguth, H.,
740 Nussbaumer, S. U., Gärtner-Roer, I., Thomson, L., Paul, F., Maussion, F., Kutuzov, S. and Cogley,
741 J. G.: Global glacier mass changes and their contributions to sea-level rise from 1961 to 2016,
742 Nature, 568(7752), 382–386, doi:10.1038/s41586-019-1071-0, 2019.

743

https://doi.org/10.5194/tc-2020-107
Preprint. Discussion started: 8 June 2020
© Author(s) 2020. CC BY 4.0 License.

744

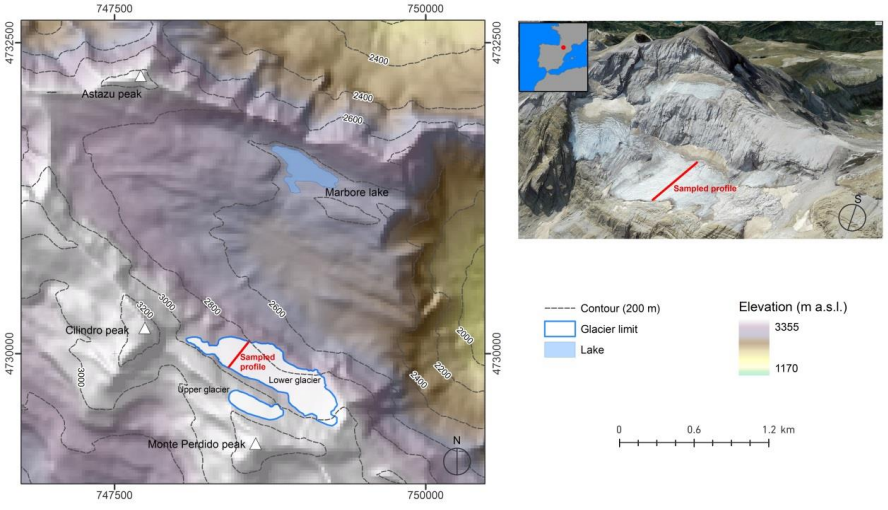

745

746

747 **Figure 1**. (left) Location of Monte Perdido Glacier (MPG) within a digital elevation map
748 of Marboré Cirque. (right) Picture (©Google Earth) of MPG where the location of the
749 samples is indicated. Note the different orientation of both figures.

750

https://doi.org/10.5194/tc-2020-107
Preprint. Discussion started: 8 June 2020
© Author(s) 2020. CC BY 4.0 License.

751

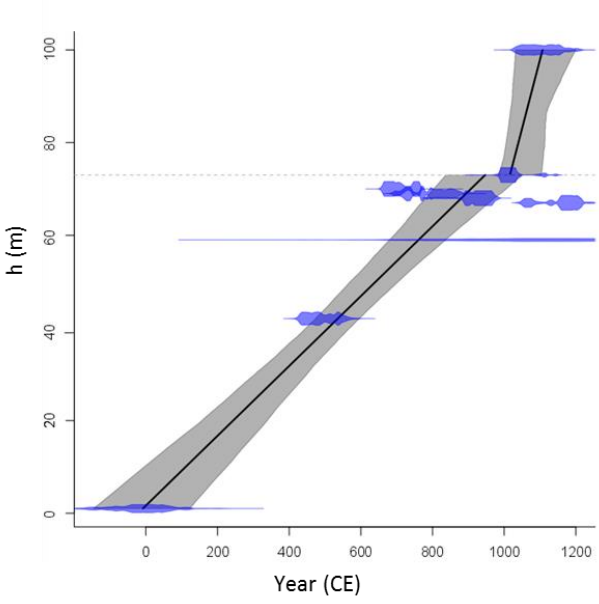

752

753 **Figure 2**. Composite depth-age model for the Monte Perdido ice sequence based on
754 linear interpolation of ^{14}C data (Table 1), obtained using the Clam software (Blaauw,
755 2010; Blaauw et al., 2019). The dates appear as the calendar-age probability
756 distributions in blue, while the black line is the resulting depth-age model and the gray
757 envelope shows the 95% confidence interval. Note the hiatus located at 73m indicated
758 by a dashed line.

759

https://doi.org/10.5194/tc-2020-107
Preprint. Discussion started: 8 June 2020
© Author(s) 2020. CC BY 4.0 License.

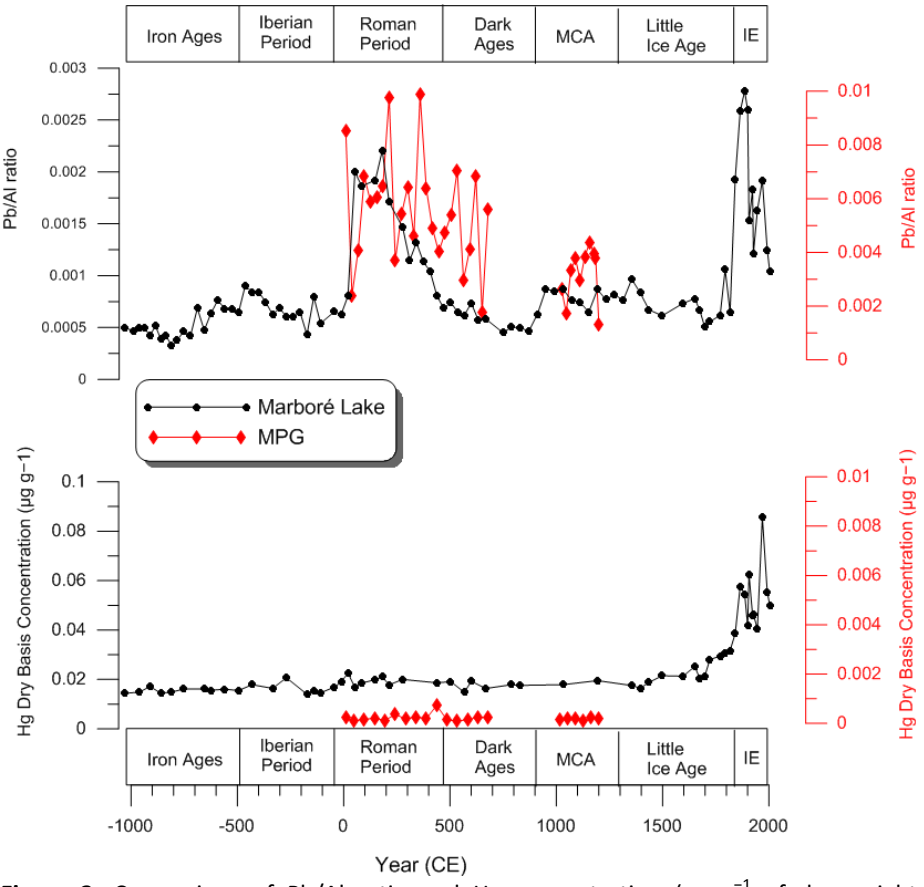

Figure 3. Comparison of Pb/Al ratio and Hg concentration (µg g^{-1} of dry weight sediment) in MPG samples with data obtained from Marboré Lake sediments (Corella et al., 2020). Note the differences in the vertical axis.

https://doi.org/10.5194/tc-2020-107
Preprint. Discussion started: 8 June 2020
© Author(s) 2020. CC BY 4.0 License.

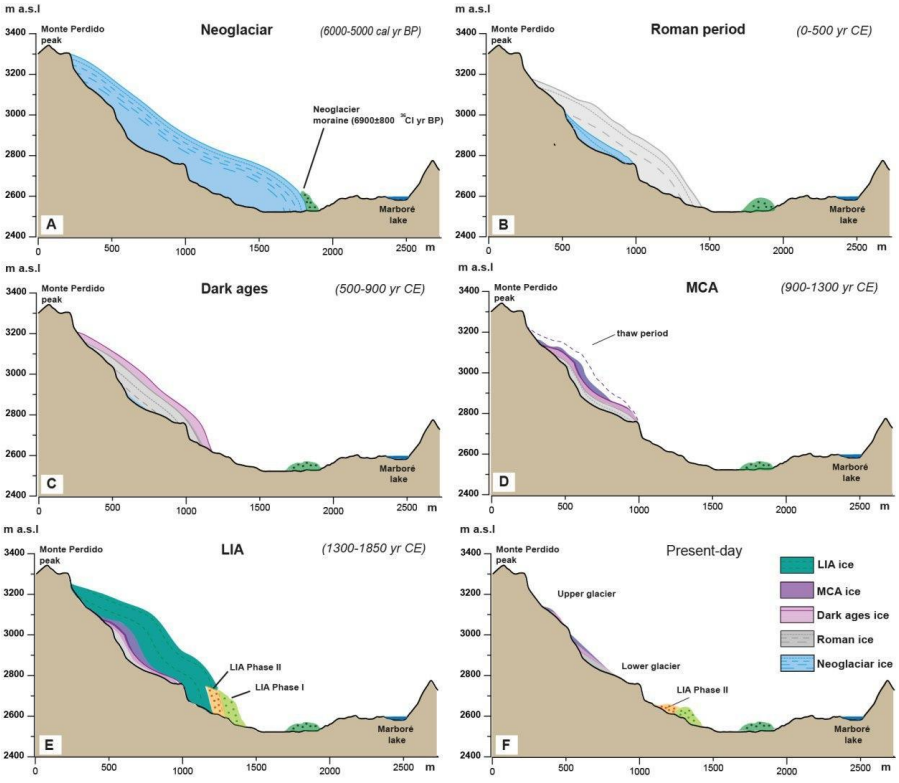

765

766 **Figure 4.** Geomorphic transects (south to north) taken from the Marboré Cirque,
767 showing the schematic reconstruction of MPG during the six main stages discussed in
768 the text. A) Neoglacial Period (ca 5000 – 6000 cal yr BP) where the Neoglacial moraine
769 is indicated (García-Ruiz et al., 2014); (B) Roman Period (0-500 CE) when the glacier is
770 shown considerably retreated; (C) Dark Ages (500-900 CE); (D) Medieval Climate
771 Anomaly (900-1300 CE), a period when the glacier retreated and ablation made
772 condensing debris and organic remains form dark layers in the glacier ice
773 (discontinuous line aims to highlight the importance of melting processes); (E) Little Ice
774 Age (1300-1850 CE), with the MPG reaching the LIA moraines position and (F) present-
775 day situation characterized by the MPG divided into two ice bodies, no ice remaining
776 from the LIA, and very steep slopes.

777

https://doi.org/10.5194/tc-2020-107
Preprint. Discussion started: 8 June 2020
© Author(s) 2020. CC BY 4.0 License.

The Cryosphere Discussions
Open Access
EGU

778 **Table 1.** Radiocarbon dating of MPG samples indicating their origin, the radiocarbon
779 age (^{14}C age BP) and the calibrated date using INTCAL13 curve and presented in
780 calendar years Common Era (CE). Samples in red and *italics* were not included in the
781 age model (see text for explanation).

Laboratory ID	Sample depth (m from base)	Sample description	^{14}C age BP	Cal age (CE)
D-AMS 025291	1	Bulk organic matter	2000±64	8±66
MP10m	10	WIOC	812±755	*854±721*
D-AMS 031464	30	pollen concentration	3906±42	*-2384±1332*
D-AMS 025294	42	bulk organic matter	1554±27	462±32
D-AMS 025295	48	bulk organic matter	73±33	*1897±20*
MP59m	59	WIOC	926±268	1046±242
D-AMS 025296	67	bulk organic matter	876±29	1185±31
D-AMS 029894	67	bulk material (filter)	485±40	*1429±15*
D-AMS 026592	68	bulk organic matter	1128±22	942±24
D-AMS 026593	69	bulk organic matter	1230±23	730±14
D-AMS 025297	70	bulk organic matter	1308±28	680±16
D-AMS 031465	70	pollen concentration	1787±37	*237±255*
D-AMS 025298	73	bulk organic matter	1011±25	1012±16
D-AMS 033972	81	bulk material (filter)	1758±25	*287±68*
D-AMS 025299	100	bulk organic matter	923±39	1074±31
D-AMS 031466	100	pollen concentration	1854±30	*158±807*

782

https://doi.org/10.5194/tc-2020-107
Preprint. Discussion started: 8 June 2020
© Author(s) 2020. CC BY 4.0 License.

783 **Table 2.** Elemental concentration (ppm) of major and trace metals in both Ordesa's
784 current deposited dust and MPG ice deposits (averaged values for the 35 analyzed
785 samples); Upper Crust elemental contents (Taylor and McLennan, 1995); and Al-
786 normalised Enrichment Factors (EF) for dust components and elements for: Ef_i, the
787 MPG ice dust versus the current Ordesa's deposited dust (CODD); EF_{iCODD}, the CODD
788 versus the Upper Crust (UC); and EF_{iMPGID}, the MPG ice dust versus the UC.

Ordesa 2016-2017 (2 years atmospheric deposition)				Monte Perdido (ice dust: 35 filter samples)				U. Crust	Enrichment Factors			
ppm	Max	Min	Average	1mg dust	Max	Min	Average		EF_i	EF_{iCODD}	EF_{iMPGID}	
OC	443270	49659	206814	**OC**	436343	14793	126381		0,4			OC
EC	114519	12506	39995	**EC**	112769	14668	40605		0,6			EC
Al	122401	7883	60410	**Al**	506467	19611	98808	80400	1,0	1,0	1,0	Al
Ca	22578	3182	9663	**Ca**	119648	256,7	11984	30000	0,8	0,4	0,3	Ca
Fe	63218	2901	32665	**Fe**	183957	12504	59477	35000	1,1	1,2	1,4	Fe
K	27478	3907	14839	**K**	57038	4001	18505	28000	0,8	0,7	0,5	K
Mg	27286	2105	12265	**Mg**	72210	3513	16645	13300	0,8	1,2	1,0	Mg
Na	5380	1,2	1413	**Na**	25750	593	5126	28900	2,2	0,1	0,1	Na
Ti	5035	257	2334	**Ti**	52192	3243	13662	3000	**3,6**	1,0	**3,7**	Ti
Mn	1656	128	582	**Mn**	3835	174	979	600	1,0	1,3	1,3	Mn
Sr	170	19	78	**Sr**	200	20	80	350	0,6	0,3	0,2	Sr
Be	7	0	2,1	**Be**	2,3	0	0,4	3	0,1	0,9	0,1	Be
V	208	10	76	**V**	257	28	107	60	0,9	1,7	1,5	V
Cr	720	5	118	**Cr**	2915	12	441	35	**2,3**	**4,5**	**10,3**	Cr
Co	32	0	7,6	**Co**	49	5,4	20	10	1,6	1,0	1,6	Co
Ni	414	7	55	**Ni**	1046	4,3	228	20	**2,5**	**3,6**	**9,3**	Ni
Cu	683	33	127	**Cu**	26451	92	3786	25	**18,3**	**6,7**	**123,2**	Cu
Zn	9391	164	1316	**Zn**	3826	171	988	71	0,5	**24,7**	**11,3**	Zn
As	26	2	10	**As**	51	5,3	18	1,5	1,0	**9,1**	**9,6**	As
Se	90	0	22	**Se**	30	0	5,2	50	0,1	0,6	0,1	Se
Cd	100	0	14	**Cd**	1,5	0	0,3	0,98	0,0	**18,8**	0,2	Cd
Sb	26	0	4,5	**Sb**	59	2	11	0,2	1,5	**29,7**	**43,3**	Sb
Ba	1010	15	287	**Ba**	870	67	317	550	0,7	0,7	0,5	Ba
Tl	1	0	0,1	**Tl**	1,1	0	0,2	0,75	1,7	0,1	0,2	Tl
Pb	175	8	53	**Pb**	2989	86	495	17	**5,7**	**4,2**	**23,7**	Pb
Th	37	1	12	**Th**	26	1,6	9,7	10,7	0,5	1,5	0,7	Th
U	8	0	2,5	**U**	15	0	3,7	2,8	0,9	1,2	1,1	U

789